Available online at www.sciencedirect.com

ScienceDirect

Procedia CIRP 58 (2017) 623 – 628

www.elsevier.com/locate/procedia

Modeling thread milling forces in mini-hole in dental metallic materials

Anna Carla Araujo[a], Guillaume Fromentin[b]

[a]*Mechanical Engineering Department - Poli/COPPE/UFRJ, Brazil*
[b]*LABOMAP - ENSAM/Cluny, France*

* Corresponding author. Tel.: +55-21-3938-7498 *E-mail address:* anna@ufrj.br

Abstract

Thread milling processes produces lower forces and residual stresses if compared to thread cutting by turning, as the cutting area is lower because the feed rate is not dependent to the cutting speed. In industry, internal threads on the abutments for metallic dental implant are usually produced by turning, although thread milling could be an alternative choice. In this article, thread milling is used to manufacture internal threads in two metallic dental materials: Titanium alloy and Cr-Co alloys, using the M2 thread geometry typical of those elements. Commercial tool is used and the relation with machined geometry is analyzed. It is concluded that the small tool diameter/internal diameter ratio impacts on the reduced steady state region compared with the region affected by penetration. The specific cutting forces were found similar in both materials using two feed rates, for three initial depth of cut and same cutting speed and identical thread geometry, considering the maximum value per revolution.

Peer-review under responsibility of the scientific committee of The 16th CIRP Conference on Modelling of Machining Operations

Keywords: Thread milling; Cutting Force; Dental Implants; Titanium Alloy; Cr-Co Alloy

1. Introduction

Typically, two biocompatible metal groups are used in dentist industry: using titatium (commercially pure CP-Ti and Ti Alloys), as per its corrosion resistance and a high strength-to-weight ratio [1,2], and crome cobalt alloys, having sufficient strength to withstand the occlusal forces applied to partial denture frameworks [3]. Implants geometries usually includes external or internal threads where it can be a weak region for the structure. If the geometry cannot be adapted, manufacturing process could change to reduce the problem. [4] studied internal threads in implantes that failed catastrophically after 6 months of service is due to a fracture presented at the inner screw used for fixation of the abutment. Elias [5] simulated the internal threaded connection on implant abutment in a dental application. One example of implants using internal threads is presented in Fig. 1 [2].

Thread milling is used to manufacture internal threads for hard materials, as Ti-6Al-4V and Cr-Co. The cutting process produces much lower residual stress and it can solve the problem studied by Hernandez [4], where the rough surface finish found in the screw and the concentration factor by geometry change caused a crack which was propagated until the failure. It is a complex machining technique that presents an elaborated tool geometry and an helical tool trajectory [6]. The force modeling for this manufacturing process presents deep analysis of geometry and kinematics[7,8,9,10,11].

The aim of this article is to compare thread milling cutting forces of mini-threads in two different biomaterials are used in experiments: commercial Ti-6Al-4V and *Romur 400*, a dental Cr-Co alloy. Experiments are realized to determine the specific cutting force and for prediction of cutting forces in implants. The modeling of forces can be used to preview residual stress and design better implants.

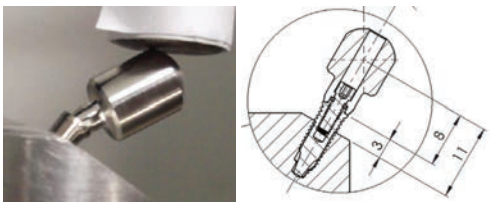

(a) Picture (b) Geometry

Fig. 1. Implant internal threaded connection on abutment [2]

Peer-review under responsibility of the scientific committee of The 16th CIRP Conference on Modelling of Machining Operations
doi:10.1016/j.procir.2017.03.228

2. Thread Milling Process

Previous articles describe and analyze completely the basic of the thread milling process [7,12]. Drilling geometry produces the initial inner diameter D_1 for thread milling. The thread milling begins the cutting trajectory centralized in O, as shown in Fig. 2a. The penetration strategy to enter into the bulk is a half revolution penetration (HRP) from point O to point A in Fig. 2b. After this stage, the "full machining" (FM) trajectory produces an internal thread geometry using the helical path: r_{tt} radius tool trajectory (XY projection plane in Fig. 3a) and going up (for right hand thread and down milling) a distance equals to the pitch P in Z direction, inside the drilled hole (from A back to A). After machining, the tool goes back to the center without removing material.

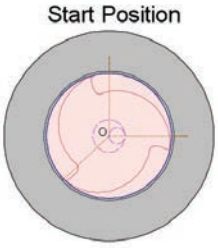

(a) Tool centered in O

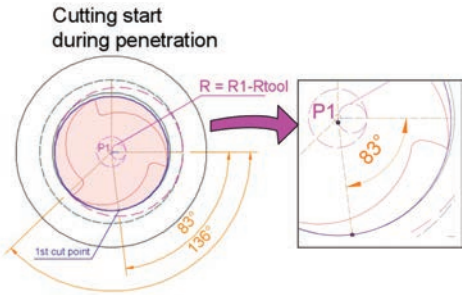

(b) Tool centered in P1

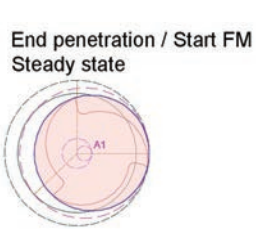

(c) Tool centered in A1

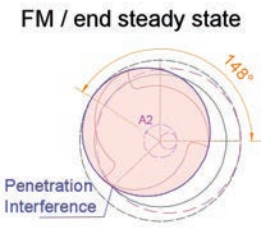

(d) Tool centered in A2

Fig. 2. Analysis of penetration on thread milling (M2 configuration)

Each tool cutting edge is composed by thread profile and there are three different orientations per section: upper orientation (faced to z+), front (as a regular end milling) and lower orientation (faced to z-). The uncut chip thickness shown in Fig. 4 for FM is the one calculated considering the front cutting edge.

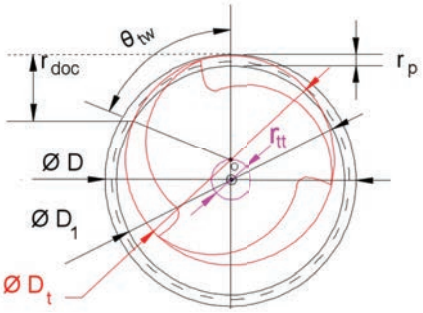

(a) Geometrical thread milling parameters

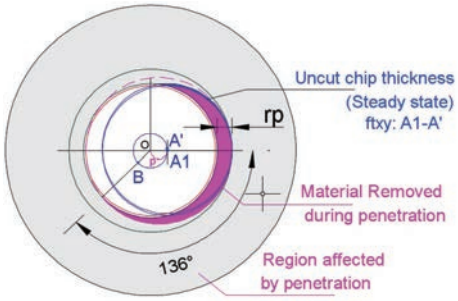

(b) Uncut chip thickness during Steady State

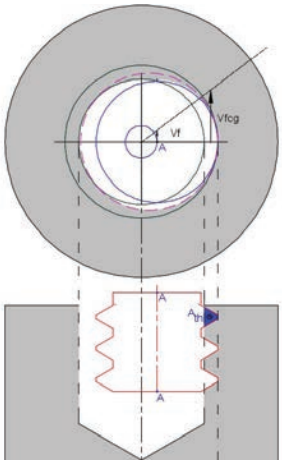

(c) Area removed per thread in z direction

Fig. 3. Thread Milling Trajectory [11]

Three referential frames are important while analyzing thread milling forces: R_0, R_1 and R_2, as shown in Figure 2.1.

The fixed referential R_0 is located in the center of the machined hole and oriented by the machine axis. The tool axis coordinates x, y and z and the forces F_x, F_y, F_z are written in R_0. The tool axis position in XY plane defines $\theta_1 = \arctan(y/x)$ and locates R_1.

The referential frame R_1 moves with the tool axis while it describes the helical trajectory, as shown in Figure 4. The local interaction between the tool and the machined surface are described by forces F_{rad} and F_{tan}, radial and tangent to the drilled surface, written in R_1. The referential frame R_2 is fixed in the tool center oriented by one fixed point in one cutting edge. Tool rotation angle θ_2 is positive to the clockwise direction.

The cutting force $\vec{F_{res}}$ can decomposed in the described referential frames. In this article, dynamometer forces are measured in the referential frame R_0. Equation 1 is used to transform measured forces to the force components in R_1. Resultant force magnitude is also analyzed F_r in this article (Eq.2).

$$\overrightarrow{F_{res}} = \begin{bmatrix} F_{rad} \\ F_{tan} \\ F_z \end{bmatrix} = \begin{bmatrix} \cos(-\theta_1) & -\sin(-\theta_1) & 0 \\ \sin(-\theta_1) & \cos(-\theta_1) & 0 \\ 0 & 0 & 1 \end{bmatrix} \begin{bmatrix} F_x \\ F_y \\ F_z \end{bmatrix} \quad (1)$$

$$F_{res} = \sqrt{(F_x^2 + F_y^2 + F_z^2)} \quad (2)$$

2.1. Thread Milling Parameters

In full machining, the tool has two important engagement parameters related to circular trajectory in xy plane: radial penetration r_p (Eq.3) and radial depth of cut r_{doc} (Eq.4) [10], calculated using the nominal thread diameter D, minor diameter of the internal thread D_1 [13], thread pitch and the tool diameter D_t. The vertical engagement parameter called axial depth of cut a_{doc}, as in end milling. In thread milling, it is a function of θ_1, pitch and the initial depth of cut a^o_{doc} as the tools move vertically (sinal "-" in Fig. 5 indicates that the tool is going up). For a metric thread, those parameters are calculated by:

$$r_p = (D - D_1)/2 \quad (3)$$

$$r_{doc} = \frac{P(80.\sqrt{3}D - 75.P)}{256(D - D_t)} \quad (4)$$

$$a_{doc}(\theta_1) = a^o_{doc} - \frac{\theta_1}{360^o}.P \quad (5)$$

Feed per tooth f_t takes into account the helical trajectory, it can be projected to the XY plane $f_{t_{xy}}$,calculated using the angular thread pitch p_θ [10], and in vertical direction f_{t_z}.

$$f_{t_{xy}} = f_t.\left(\left(\frac{p_\theta}{r_{it}}\right)^2 + 1\right)^{-0.5} \quad (6)$$

$$p_\theta = P/2\pi \quad (7)$$

$$f_{t_z} = \sqrt{f_t^2 - f_{t_{xy}}^2} \quad (8)$$

Based on the tool flute angle λ_{st}, it is calculated the the flute engagement angle δ that in thread milling depends to tool position (θ_1).

$$\delta(\theta_1) = a_{doc}(\theta_1).\frac{2.\tan(\lambda_{st})}{D_t} \quad (9)$$

Cutting continuity coefficient c quantifies the relative number of flutes simultaneously in contact with the workpiece, the tool engagement in the workpiece. In thread milling, c is a function of θ_1, of the angle between flutes is $\theta_f = \frac{2\pi}{N_f}$ for N_f flutes and tooth working angle θ_{tw} [12].

$$c(\theta_1) = \frac{\delta(\theta_1) + \theta_{tw}}{\theta_f} \quad (10)$$

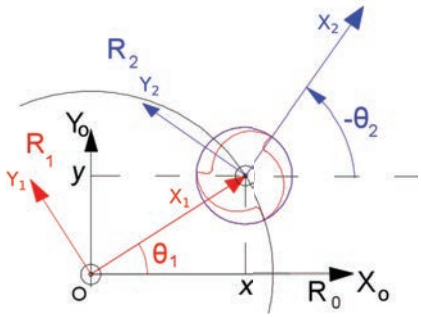

Fig. 4. Referential Frames R_0, R_1 and R_2

2.2. Specific Cutting Force

Cutting force models are commonly expressed as a function of uncut chip area A_c and specific cutting force K_c[14].

$$F_c = K_c.A_c \quad (11)$$

If cutting continuity is less than one, only one thready cutting edge is cutting at any instant, so the cutting power can be approximated by average resultant force F^{Av}_{res} per cutting edge and the cutting speed V_c (m/min). The specific cutting forces K_P (using subindex 'P" that indicates it is calculated using cutting power - P_c [N.m/min]) is then a function of the material removal rate MRR (mm^3/min):

$$P_c \approx F^{Av}_{res}.V_c \rightarrow K_P = \frac{P_c}{\text{MRR}} = \frac{F^{Av}_{res}.1000.V_c}{\text{MRR}} \quad (12)$$

As presented in [11], for thread milling the material removal rate is a function of the cutting thread area $A_t h.a_{doc}$ and the feed rated on the gravity center of the removed material V^{gc}_f in (mm/min) (Figure 3(c)):

$$MRR = V^{gc}_f.\frac{A_{thr}.a_{doc}}{P} \quad (13)$$

So, the specific cutting force $K_T$is calculated by Eq. 14. (C^* is constant for a specific experiment (f_t constant) and k^P (N/mm) represents the cutting force divided by the instantaneous depth

of cut, that can be calculated based on the experimental data.

$$K_P = \frac{F_{res}^{Av}.1000.V_c.P}{V_f gc.A_{thr}.a_{doc}} = k_P.\frac{1000.V_c.P}{V_f^{gc} A_{thr}} = k_P.C^* \quad (14)$$

$$k_P = \frac{F_{res}^{Av}}{a_{doc}} \quad (15)$$

3. Materials and Methods

The experiments used two different materials using the same cutting geometry: titanium alloy Ti6Al4V workpiece and *Romur 400*, a dental Cr-Co alloy, with water based emulsion. The Cr-Co alloy chemical composition is: 62.5% Co 28.5% Cr 6.1% Mo 0.55% Mn, typically it has: yield stress (0.2%) to 705 MPa, 2.6% elongation in fracture, and elastic modulus 185 GPa.

3.1. Cutting Parameters

The design of experiments is presented in Table 3.1. Two different feed were chosen and three initial depth of cut, cutting speed is constant for all experiments. Three replica was used for each experiment. Thread milling run-out was measured to assure levels below 0.01 mm. The materials were drilled using

Table 1. Design of Experiments for Cr-Co and Ti6Al4V

Experiment	f_t (mm/th)	a_{doc}(mm)
A	0.025 (L)	1.2 (3P)
B	0.035 (H)	1.2 (3P)
C	0.025 (L)	0.8 (2P)
D	0.035 (H)	0.8 (2P)
E	0.025 (L)	0.4 (1P)
F	0.035 (H)	0.4 (1P)

a Mitsubishi tool: MWS0160SB with 1.6 mm diameter. The drilled hole had 4 mm height (2.8 mm vertical clearance for the deeper experiment). The geometry of threads are metric M2 and right hand. The thread milling tool geometry is H5087006-M2 manufactured by Walter Co, called commercially "Orbital Thread Mills", that produces threads pitch by pitch in a helical operation, to produce a M2x0.4mm. It is a solid carbide coated (TiCN). The tool geometry is: 15^o helix angle, $P = 0.4mm$, cutting edge diameter $D_t = 1.55mm$ and spindle speed $n = 4110rpm$). The tool has three thready cutting edges ($N_f = 3$). The manufactured recommendation is using radial penetration equals to $r_p = 0.2mm$. The thread milling cutting parameters in these experiments were: $p_\theta = 0.0637$, $r_{doc} = 0.8581$mm, $\theta_{tw} = 90^o$, $\theta_f = 120^o$, $A_{th} = 0.02625mm^2$. Cutting continuity $c(\theta_1)$ is for three cases (P, 2P and 3P) and presented in Fig. 4. It was chosen half penetration strategy.

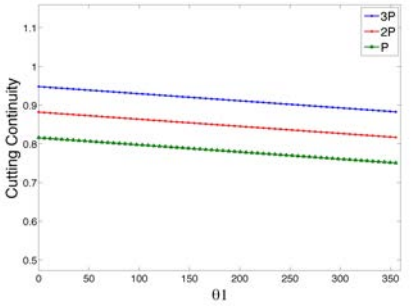

(a) Cutting continuity

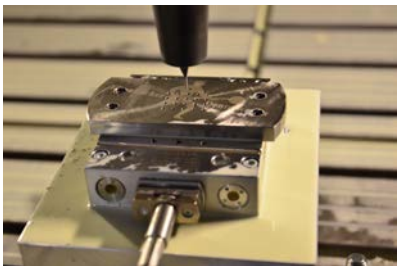

(b) Thread milling forces acquisition

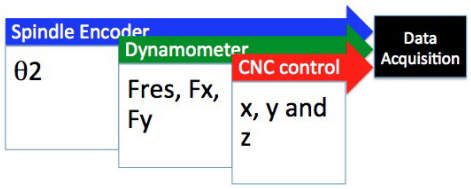

(c) Acquisition Configuration

Fig. 5. Experimental data acquisition

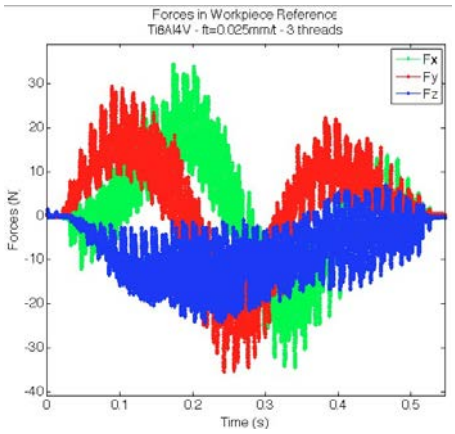

(a) Acquired Forces (R_0 Reference frame)

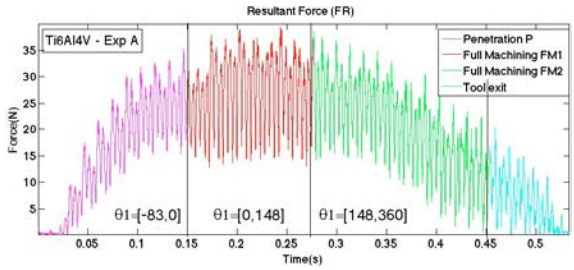

(b) Resultant Force F_{res} - three regions: P+FM1+FM2

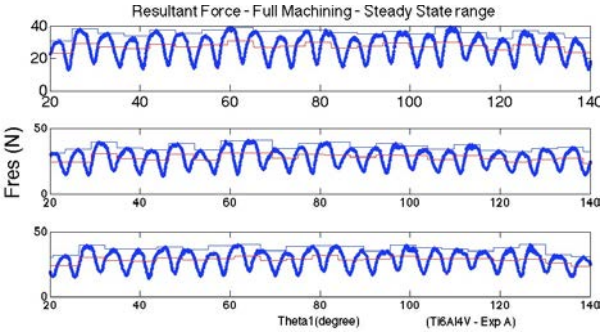

(c) Resultant Force F_{res} in FM1 and Average per Revolution

Fig. 6. Thread Milling Forces (Experiment A - Ti6Al4V)

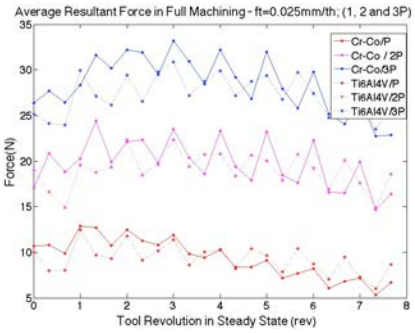

(a) F_{res}^{Av} $(ft = 0.025mm/th)$

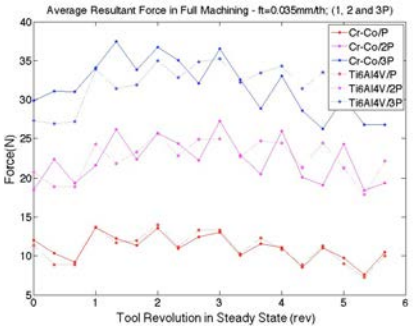

(b) F_{res}^{Av} $(ft = 0.035mm/th)$

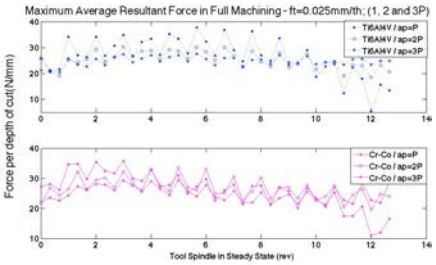

(c) k_P (N/mm^2) $(ft = 0.025mm/th)$

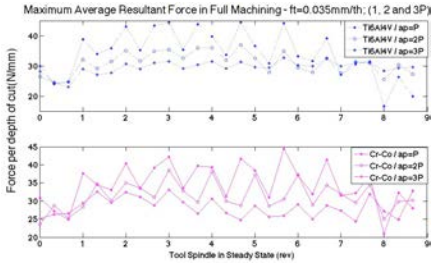

(d) k_P (N/mm^2) $(ft = 0.035mm/th)$

Fig. 7. Average resultante Force per cutting edge and forces per depth of cut for Cr-Co and Ti6Al4V

3.2. Data Acquisition

Continuous data acquisition is carried out: cutting forces, tool axis positions (X, Y and Z) and tool angle position A high band width and sensitive dynamometer (Kistler MiniDyn 9256C2) is used for cutting force data acquisition. A CNC machining center DMC85VL is used for all experiments. Tool axis position (x, y and z) were read from CNC analog output in order to determine θ_1. The incremental spindle encoder is used to measure θ_2 tool angle position. A National Instruments data board acquisition is used with DasyLab software for data treatment. In this article, only full machining without penetration influence is considered ($0 < \theta_1 < 148^o$). Effectivity, due to a tool diameter close to the $D1$ thread diameter, an 136^o angular region of the thread is already machined during the tool penetration, from $\theta_1 = -83^o$ to 0^o position, as shown on Fig 2(b). The FM steady state starts when tool center position is at point A2, $\theta_1 = 0^o$ Fig 2(c), and continues until it reaches A2 point, $\theta_1 = 148^o$, Fig 2(c). In this last position, the tool envelope joins the thread region initially affected by the tool penetration. As a consequence, the same θ_1 range, from 0 to 148^o, was used to guarantee the same axial depth of cut range and a proper the comparison of forces during the FM steady state .

4. Experimental Results

All the force data acquired is taken in R_0 reference frame, as shown in Fig. 6(a), and F_{res} is calculated identifying the three regions: penetration (P), full machining without penetration influence (FM1) and full machining with penetration influence (FM2) as it can be observed on Fig. 6(b). This graphic presents an example of data, experiment (A) machining Titanium alloy. It can be observed that after FM2, there is non expected forces acting on the tool. One possibility is tool deflection during penetration during FM.

The three replicates were taken into account, considering θ_1 position for all experiments. The average resultant forces is computed on each threaded cutting edge passing (3 per revolution) as shown in Fig. 6(c). Computing for all tests and experiments, Fig. 7(a) presents all average resultant forces F_{res}^{Av} for the lower feed rate ($f_t = 0.025mm/th$) and Fig. 7(b) for $f_t = 0.035mm/th$. As expected, as the number of threads increases, the force is higher, it can be seen three different curves for each initial depth of cut. In other hand, there is no difference between the experienced materials. Also, feed rate in this range does not affect the average resultant force.

In order to analyze the specific cutting force, it is calculated the instantaneous depth of cut for every revolution and the cutting load per depth of cut is computed. The influence of the depth of cut is taken out in analyzing k_P. In Fig. 7(c) the lower feed rate, k_P is slightly lower the in Fig. 7(d), as expected.

5. Conclusions

This article deals with thread milling process to manufacture mini-hole M2 in two dental materials. The geometrical analysis of the thread milling process and a mechanistic modelling of cutting force in relation with experiments are proposed and some conclusion can be claimed:

- Using comercial tools, the difference between tool diameter and hole diameter is too small, increasing the area affected by penetration. This situation is not good for thread quality because induce change in tool deflection.
- The appearance of forces after FM finished shows that the material was under machined in the beginning of thread milling process.
- Average resultant forces in the feed rate levels on both materials analyzed are not significantly different.
- In order to compare the machinability of the materials, the average force divided by the depth of cut is calculated in both materials and the results shown similar values.
- Deeper analysis can be done with instantaneous cutting force in R1 and R2 referential frames in the future.

Acknowledgement

The authors would like to acknowledge CNPq for the research resources on Edital Universal project 481406/ 2013-1.

References

[1] J. Lee, S. Hurson, H. Tadros, P. Schupbach, C. Susin, U. Wikesjo, Crestal remodelling and osseointegration at surface- modified commercially pure titanium and titanium alloy implants in a canine model, Journal of Clinical Periodontology 39 (2012) 781–788.
[2] C. N. Elias, D. J. Fernandes, C. R. Resende, J. Roestel, Mechanical properties, surface morphology and stability of a modified commercially pure high strength titanium alloy for dental implants, Dental Materials 31 (2) (2015) e1 – e13.
[3] M. McCracken, Dental implant materials: Commercially pure titanium and titanium alloys, Journal of Prosthodontics 8 (1) (1999) 40–43.
[4] M. Hernandez-Rodriguez, G. Contreras-Hernandez, A. Juarez-Hernandez, B. Beltran-Ramirez, E. Garcia-Sanchez, Failure analysis in a dental implant, Engineering Failure Analysis 57 (2015) 236 – 242.
[5] C. N. Elias, J. Lima, R. Valiev, M. Meyer, Biomedical applications of titanium and its alloys, Biological Materials Science March (2008) 46–49.
[6] G. Fromentin, B. Dobbeler, D. Lung, Computerized simulation of interference in thread milling of non-symmetric thread profiles, Procedia CIRP - 15th CMMO 31 (2015) 496 – 501.
[7] A. C. Araujo, G. M. Mello, F. G. Cardoso, Thread milling as a manufacturing process for {API} threaded connection: Geometrical and cutting force analysis, Journal of Manufacturing Processes 18 (2015) 75 – 83.
[8] M. Wan, Y. Altintas, Mechanics and dynamics of thread milling process, International Journal of Machine Tools and Manufacture 87 (2014) 16 – 26.
[9] G. Fromentin, G. Poulachon, Geometrical analysis of thread milling—part 1: evaluation of tool angles, The International Journal of Advanced Manufacturing Technology 49 (1) (2010) 73–80.
[10] G. Fromentin, G. Poulachon, Geometrical analysis of thread milling—part 2: calculation of uncut chip thickness, The International Journal of Advanced Manufacturing Technology 49 (1) (2010) 81–87.
[11] A. C. Araujo, G. Fromentin, G. Poulachon, Analytical and experimental investigations on thread milling forces in titanium alloy, International Journal of Machine Tools and Manufacture 67 (2013) 28 – 34.
[12] V. Sharma, G. Fromentin, G. Poulachon, R. Brendlen, Investigation of tool geometry effect and penetration strategies on cutting forces during thread milling, International Journal of Advanced Manufacturing Technology (2014) p. 913 – 919.
[13] ISO, General purpose screw threads basic profile part 1 metric screw threads, ISO Standard 68 (1) (1998) 82 – 88.
[14] Y. Altintas, P. Lee, A general mechanics and dynamics model for helical end mills, CIRP Annals - Manufacturing Technology 45 (1) (1996) 59 – 64.